increases as the accessibility of the C–O skeletal bonds to gauche states increases, following the order POx > PMOx > PDOx. Assuming that the glass transition temperature of the polymers is closely related to the molecular flexibility such that the higher is the flexibility generally the lower is T_g,[32,33] the values of T_g should decrease in the order PDMOx > PMOx > POx. This prediction is confirmed in the last column of Table II, where it can be observed that the glass transition of PDMOx is higher than that of POx, the value of T_g corresponding to PMOx being intermediate.

Acknowledgment. This work was partially supported by the Comisión Asesora de Investigación Cientifica y Técnica. Thanks are due to Dr. J. L. Nieto from the Instituto de Estructura de la Materia (CSIC) for valuable comments on the ^{13}C NMR spectra. We also thank Mr. D. Delgado and Mr. J. Guisández for technical assistance.

Registry No. Poly(3-methyloxetane), 87706-57-8; PMOx, 90697-51-1.

References and Notes

(1) Rose, J. B. *J. Chem. Soc.* **1956**, 546.
(2) Okamura, S. *Encycl. Polym. Sci. Technol.* **1968**, *9*, 668.
(3) Saegusa, T.; Fujii, H.; Kobayashi, H.; Ando, R. *Macromolecules* **1973**, *6*, 26.
(4) Bucquoye, M.; Goethals, E. J. *Makromol. Chem.* **1978**, *179*, 1681.
(5) Abe, A.; Mark, J. E. *J. Am. Chem. Soc.* **1976**, *98*, 6468.
(6) Takahashi, Y.; Mark, J. E. *Polymer* **1976**, *17*, 670.
(7) Garrido, L.; Riande, E.; Guzmán, J. *J. Polym. Sci., Polym. Phys. Ed.* **1982**, *20*, 1805.
(8) Saiz, E.; Riande, E.; Guzmán, J.; de Abajo, J. *J. Chem. Phys.* **1980**, *73*, 958.
(9) Chiu, D. S.; Mark, J. E. *J. Chem. Phys.* **1977**, *66*, 1901.
(10) Searles, S.; Pollart, K. A.; Lutz, E. F. *J. Am. Chem. Soc.* **1957**, *79*, 948.
(11) Garrido, L.; Guzmán, J.; Riande, E.; de Abajo, J. *J. Polym. Sci., Polym. Chem. Ed.* **1982**, *20*, 3378.
(12) Ledwith, A.; Sherrington, D. C. *Adv. Polym. Sci.* **1975**, *19*, 1.
(13) Matyjaszewski, K.; Slomkowski, S.; Penczek, S. *J. Polym. Sci., Polym. Chem. Ed.* **1979**, *17*, 2413.
(14) van Gurkon, M.; Hall, G. E. *Q. Rev. Chem. Soc.* **1968**, *22*, 14.
(15) Oguni, N.; Watanabe, S.; Maki, M.; Tani, H. *Macromolecules* **1973**, *6*, 195.
(16) Ivin, K. J.; Navratil, M. J. *J. Polym. Sci., Part A-1* **1971**, *9*, 1.
(17) Kops, J.; Hvilsted, S.; Spanggaard, H. *Macromolecules* **1980**, *13*, 1058.
(18) Oguni, N.; Hyoda, J. *Macromolecules* **1980**, *13*, 1687.
(19) Riande, E.; de la Campa, J. G.; Guzmán, J.; de Abajo, J. *Macromolecules*, in press.
(20) Guggenhein, E. *Trans. Faraday Soc.* **1949**, *45*, 714; **1951**, *47*, 573.
(21) Smith, J. W. *Trans. Faraday Soc.* **1950**, *46*, 394.
(22) McClellan, A. L. "Tables of Experimental Dipole Moments", Vol. I, W. H. Freeman: San Francisco, 1963; Vol. II, Rahara Enterprises: El Cerrito, CA, 1974.
(23) Riande, E.; Boileau, S.; Hemery, P.; Mark, J. E. *J. Chem. Phys.* **1979**, *71*, 4206.
(24) Riande, E.; Boileau, S.; Hemery, P.; Mark, J. E. *Macromolecules* **1979**, *12*, 702.
(25) Marchal, J.; Benoit, H. *J. Polym. Sci.* **1957**, *23*, 223.
(26) Nagai, K.; Ishikawa, T. *Polym. J.* **1971**, *2*, 416.
(27) Doi, M. *Polym. J.* **1972**, *3*, 352.
(28) Liao, S. C.; Mark, J. E. *J. Chem. Phys.* **1973**, *59*, 3825.
(29) Flory, P. J. "Statistical Mechanics of Chain Molecules"; Wiley: New York, 1969.
(30) Flory, P. J. *Macromolecules* **1974**, *7*, 381.
(31) Riande, E.; García, M.; Mark, J. E. *J. Polym. Sci., Polym. Phys. Ed.* **1981**, *19*, 1739.
(32) Tonelli, A. E. *Macromolecules* **1974**, *7*, 632.
(33) Tonelli, A. E. *Macromolecules* **1977**, *10*, 633, 636.
(34) Willbourn, A. H. *Trans. Faraday Soc.* **1958**, *54*, 717.
(35) Saba, R. G.; Sauer, J. A.; Woodward, A. E. *J. Polym. Sci., Part A-1* **1963**, 1483.
(36) Faucher, J. A.; Koleske, J. V. *Polymer* **1968**, *9*, 44.
(37) Garrido, L.; Guzmán, J.; Riande, E. *Makromol. Chem., Rapid Comm.* **1983**, *4*, 725.
(38) Pérez, E. Doctoral Thesis, University of Madrid, 1982.

Measurement of the Kinetics of Chain Polymerization of Single Poly(vinyl acetate) Molecules in a Cloud Chamber

Mohiuddin A. Chowdhury, Howard Reiss,* David R. Squire,† and Vivian Stannett†

Department of Chemistry and Biochemistry, University of California, Los Angeles, California 90024. *Received June 24, 1983*

ABSTRACT: The gas-phase, photoinduced, free radical polymerization of vinyl acetate is studied, using drop formation in supersaturated vinyl acetate vapor in a diffusion cloud chamber as a detector. A detailed kinetic mechanism involving initiation, propagation, termination, and chain transfer is postulated, and the corresponding rate equations are solved. We are able to achieve conditions such that growing polymer molecules cannot encounter one another. Thus the arrival, by growth, of individual polymer molecules is detected. The system can be "tuned" to detect polymer molecules of a given size by adjusting the supersaturation and therefore constitutes a technique of high resolution. In view of the "extreme" nature of the measurement, no alternative method exists that allows a comparative confirmation of the assumed fundamental process. Therefore, confirmation is a "bootstrap" operation in which the harmonious register of many quantitative and qualitative observations, with each other and with theory, must be used to prove-out the technique. The demonstration of this observational consistency, and *not* the measurement of particular kinetic parameters, forms the main purpose of this paper. Almost all the features of the assumed kinetic mechanism are dramatically confirmed. Detected polymer molecules have degrees of polymerization of the order of 50, and the activation energy for propagation is of the order of 4000 cal mol^{-1}, in agreement with independent studies on bulk polymerization. The "noise" in the polymerization reaction is actually sensed.

I. Introduction

In a recent paper[1] we developed a theory for the nucleation of supersaturated vapors of monomers, by polymers formed from them. Using this theory, we made quantitative estimates of the various associated phenomena for the case of vinyl acetate. The results indicated that it should be possible to achieve experimental conditions under which a single poly(vinyl acetate) molecule could nucleate the condensation of supersaturated vinyl acetate vapor. Indeed, it appeared that conditions could be

†Department of Chemical Engineering, North Carolina State University.

0024-9297/84/2217-1436$01.50/0

achieved in which *every* polymer molecule of a sharply critical size would serve as a nucleus for condensation. Stated in another way, the theory indicates that if a polymer molecule of a certain critical size appears (by whatever process) in monomer vapor having a certain degree of supersaturation, its lifetime, before the formation of a liquid drop of monomer is induced, would be of the order of a microsecond. Reducing the degree of polymerization slightly (see Table II of ref 1) increases the lifetime (for the same degree of monomer supersaturation) by many orders of magnitude.

The circumstances suggest an interesting application to the study of the mechanism of gas-phase chain polymerization. Under normal conditions the study of gas-phase polymerization is complicated by the fact that oligomers, because of their low volatility, condense out of the vapor before they develop into larger polymers. Polymer chains may continue to grow after having been deposited on the walls of the reaction vessel. Monomer from the gas continues to supply this growth, but then the process no longer strictly represents gas-phase polymerization. An obvious way to avoid this problem is to reduce the concentration of chains in the gas to a low enough level, so that oligomers cannot encounter one another. Unfortunately, this alternative carries with it the penalty that the rate of polymerization becomes exceedingly difficult to observe because of the inordinately low rate of monomer consumption. In most studies of the rate of polymerization, the speed of disappearance of monomer is employed as a measure of that rate, and, indeed, the speed of disappearance of monomer is actually *defined* as that rate.[2] The few studies of the kinetics of gas-phase polymerization which exist[3-7] have almost all relied on the measurement of gas pressure to sense the disappearance of monomer. Obviously, this technique would be difficult to apply in the circumstances mentioned above. However, the fact that the growing polymers can nucleate supersaturated monomer vapor presents another possibility.

If a single polymer molecule of the critical size can cause the formation of a liquid drop of monomer, then the appearance of that drop can be used to signal the arrival of the polymer of that size. Thus, instead of observing the disappearance of monomer, one can sense the arrival of polymer, molecule by molecule, and measure the rate of reaction in this way. The possibility even exists to "tune" to the arrival of polymer of a *specified degree of polymerization* by controlling the level of supersaturation. Thus one has the possibility of an extremely high-resolution method for studying the kinetics. Furthermore this method is not compromised by the need to have only a small number of chains growing simultaneously in the vapor, since, in principle, even a single molecule of a given size can be detected by means of the drop that it induces.

This is the technique we have developed and, as described in this paper, have applied to the vinyl acetate system. The present paper is only the initial attempt at the use of the technique and, as such, is primarily a demonstration that it is viable, i.e., that everything is happening in the expected manner, rather than an attempt to complete a deep study of the kinetics of the gas-phase polymerization of vinyl acetate. In view of the "extreme" nature of the measurement, no alternative method exists that allows a comparative confirmation of the assumed fundamental process. Therefore, confirmation is a "bootstrap" operation in which the harmonious register of many quantitative and qualitative observations, with each other and with theory, must be used to prove-out the technique. The demonstration of this observational consistency, and *not* the measurement of particular kinetic parameters, forms the main purpose of this paper.

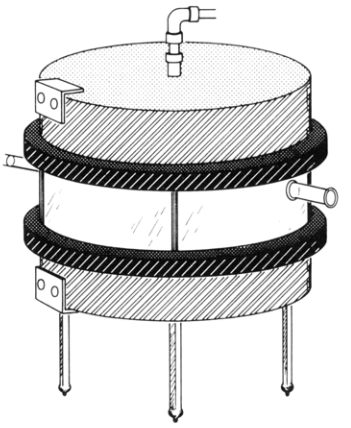

Figure 1. Schematic diagram of the cloud chamber.

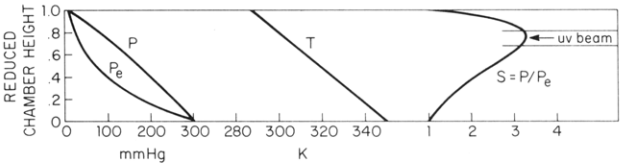

Figure 2. Example of variation of temperature T, partial pressure P, vapor pressure P_e, and degree of supersaturation S against elevation (reduced height) in the cloud chamber.

The experimental arrangement in which our measurements have been performed is the upward diffusion cloud chamber which has by now been reduced to a reliable tool for the study of vapor phase nucleation[8-11] and has also been used for the study of photochemical kinetics.[12-16] Since the method of adaptation to the study of photochemical kinetics has been described at length in ref 12–16, we will only comment on it briefly here. Figure 1 will be helpful.

The diffusion cloud chamber consists of two, horizontal, circular, metal plates separated by a glass cylinder. A shallow pool of liquid, in this case vinyl acetate, rests on the lower plate and the space between the surface of this pool and the upper plate is filled with helium. The lower plate is maintained at a temperature higher than that of the upper plate, and under these conditions vinyl acetate evaporates from the pool and diffuses through the helium gas to condense and form a smooth liquid film on the upper plate. This film drains to the side and flows down the walls of the glass cylinder to return to the pool. Convection in the helium-vapor space between the pool and the upper plate is to be avoided. Under these conditions a steady state of transport and reflux is established in the chamber in which the degree of supersaturation (defined as the ratio of the actual partial pressure of vinyl acetate to the saturation pressure corresponding to the temperature at the particular elevation in the chamber) depends on elevation, roughly in the manner indicated in Figure 2. The precise course of this curve is controlled by the temperatures of the two plates.

The polymeric reaction is initiated and maintained by a beam of ultraviolet light (indicated in Figure 2) which enters and leaves the chamber through quartz windows sealed into the glass cylinder. Polymers form by a free radical chain mechanism discussed below. By maintaining the intensity of the UV light at a sufficiently low level, one can ensure that only a small number of polymer chains will be growing simultaneously and therefore avoid the problem of the condensation of oligomers. One attempts to adjust

the horizontal position of the UV beam so that it is aimed at the maximum (see Figure 2) in the supersaturation curve. A horizontal helium–neon laser beam is positioned below the UV beam and at right angles to it. When a polymer molecule grows to the critical size necessary for it to nucleate a liquid drop of monomer at the supersaturation level involved, a drop forms and falls through the laser beam where it scatters a strong light signal to a photomultiplier in a counting circuit. In this way the number of drops (and therefore the number of molecules of critical size) formed per unit time in an optically defined volume of observation may be determined. Thus the rate of polymerization to a rather sharply defined polymer size may be measured. In the next section we discuss some of the more precise details of the experiment.

II. Experimental Section

In our experiments we found it necessary to employ silicone rubber gaskets and O-rings, because the more conventional Viton gaskets are affected by vinyl acetate, even at room temperature. The quartz windows, attached to the Pyrex glass ring through graded seals, were located at an elevation of 0.73 (reduced height) of the cloud chamber, so that the UV beam in most of our measurements remained level, approximately at the elevation where the maximum supersaturation of the vinyl acetate occurred. Both the quartz windows and several areas of the glass cylinder were kept warm by nichrome heating wires, to prevent fogging and obstruction of the UV, He–Ne laser, and the scattered laser beams. The temperatures of the top and bottom plates were measured by thermocouples located at points some 3.0 mm away from the surfaces of the plates and therefore still further away from the surfaces of both the liquid pool, on the lower plate, and the liquid film on the upper one. Ideally some of these thermocouples should be at the liquid surfaces, and so, in these experiments, the precise values of the supersaturation are not known. In subsequent experiments the thermocouples will be positioned so as to allow precise determination of supersaturation. In the present experiments the quoted supersaturations can be considerably in error. Since precise values (see below) of supersaturation are necessary in order to deduce reasonably accurate values (by the application of nucleation theory) for the various constants involved in the polymerization, the rate constants obtainable in the present experiments must be considered at best semiquantitative.

The source of UV radiation was a 1000-W xenon short-arc lamp (Oriel). A narrow beam from this lamp was passed through 10 cm of water filter in order to remove the infrared light capable of generating heat and was then collimated by passage through an optical system consisting of an iris and a 250-mm focal length quartz lens. This beam was then passed through a CS 7-54 glass filter in order to cut off all radiation of wavelength above 300 nm. The intensity of radiation in this lamp showed little variation over the duration of our experiments. The photochemical processes in the cloud chamber were actually induced by light in the narrow wavelength range 260–280 nm, because the output of the xenon lamp is negligible below 260 nm and vinyl acetate absorbs negligibly above 280 nm. A combination of neutral-density filters (Oriel, UV–vis–IR) was used to regulate the relative intensity of this radiation. The intensity of the output of the optical system without any neutral-density filter was measured with a Scientech power meter and was used as the reference intensity.

As mentioned in the previous section droplets, formed in the chamber, were detected by scattering from the beam of a He–Ne laser. Signals scattered from the laser beam at a certain narrow solid angle were amplified by means of a photomultiplier (EMI 9658R) operated at 700 V, and the pulse was sent through a current-to-voltage converter and a discriminator before entering the counter. The pulses were also observed on an oscilloscope and simultaneously integrated for a fixed time interval by the counter. The number of pulses received is displayed at the end of the time interval on a D/A converter. Figure 3 shows a typical set of counter readings for a time interval of 10 or 20 s at three different levels of UV intensity. The discriminator serves to reject the weak pulses created by a droplet falling at the edge of the laser beam. As can be seen from Figure 3 the counter readings are Poisson distributed and the average number of pulses produced per second is a measure of the rate of droplet formation. We consider this average to be proportional to the actual rate of nucleation.

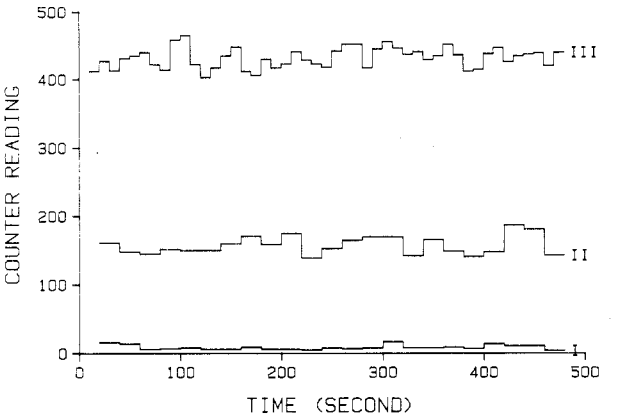

Figure 3. Plots of counter reading (total number of droplets formed in a fixed time period) against time at different light intensities: curve I, $I = 2.9 \times 10^{14}$ photons cm^{-2} s^{-1}, time period = 20 s; curve II, $I = 7.2 \times 10^{14}$ photons cm^{-2} s^{-1}, time period = 20 s; curve III, $I = 1.8 \times 10^{15}$ photons cm^{-2} s^{-1}, time period = 10 s. Elevation of the He–Ne laser beam = 0.52, $S = 1.94$, and $T = 286.3$ K (at the level of the UV beam).

As far as materials were concerned, vinyl acetate (MCB, 99.5% stated purity) was distilled twice through a 26-plate fractionating column in a nitrogen atmosphere. Only the middle fraction boiling at 72–73 °C was accepted. The final distillate was tested, using Schiff's reagent, and was found to contain no aldehyde. High-resolution mass spectrometric analysis of the sample showed no trace of impurities. The distilled product was stored in a darkened vessel with stopcock and transferred to the cloud chamber through an all-glass vacuum line provided with virgin Teflon stopcocks only. The cloud chamber was cleaned by several washings with carbon tetrachloride in order to remove solid polymer film from the plate and the glass cylinder, followed by several washings with absolute alcohol. It was then evacuated to 0.01 torr before being filled with 100 mL of vinyl acetate and 700 torr of spectroscopic-grade helium. The helium was passed through molecular sieves cooled at liquid nitrogen temperature for further purification just before its introduction into the cloud chamber. We describe experimental results in section IV after we have developed some chemical kinetic theory in section III.

III. Chemical Kinetics

We assume that the polymerization involves the standard vinyl chain reaction initiated by a free radical R· as illustrated in eq 1.

$$\mathrm{CH_2{=}CXH} + h\nu \rightarrow \mathrm{R\cdot}$$

$$\mathrm{R\cdot} + \mathrm{CH_2{=}CXH} \rightarrow \mathrm{RCH_2\text{-}\dot{C}XH}$$

$$\mathrm{RCH_2\text{-}\dot{C}XH} + \mathrm{CH_2{=}CHX} \rightarrow \mathrm{RCH_2\text{-}CXH\text{-}CH_2\text{-}\dot{C}XH}, \text{ etc.}$$

$$\mathrm{R\text{-}CH_2\text{-}(CH_2\text{-}CXH)_a\text{-}\dot{C}XH} + \mathrm{R\text{-}CH_2\text{-}(CH_2\text{-}CXH)_b\text{-}\dot{C}XH} \rightarrow \text{dead polymer} \quad (1)$$

where X is a substituent. The free radical is produced when a monomer absorbs a photon. Actually, two radicals[17] may result from this elementary absorption process, but this alternative will not change the form of the kinetic rate equations.

We will denote by R_x the concentration of polymeric free radicals of degree of polymerization x. We can express the time rate of change of the concentration of radicals of size $x = 1$ by the equation

$$dR_1/dt = k_i MI - (k_p M + k_{tr} M + k_t \theta + k_d) R_1 + k_{tr} M \theta \quad (2)$$

where

$$\theta = \sum_{i=1} R_i \tag{3}$$

and t is time. The quantities k_i, k_p, k_{tr}, k_t, and k_d are the rate constants for initiation, propagation, chain transfer, chain termination by combination, and "escape", by diffusion, from the UV beam. I is the UV light intensity, and M is the concentration of monomer. For $x > 1$, we have

$$dR_x/dt = k_pMR_{x-1} - (k_pM + k_{tr}M + k_t\theta + k_d)R_x, \qquad x > 1 \tag{4}$$

The structure of these equations may be easily understood. In eq 2 the first term on the right represents the rate of production of initial free radical chains. The last term on the right represents the rate of production of free radicals of size 1 through the process of chain transfer. The second term on the right simply expresses the loss of radicals of size $x = 1$ by all loss processes. In eq 4 the first term on the right represents the rate of increase of concentration of free radicals of size x due to propagation from radicals of size $x - 1$. The second term on the right of eq 4 again represents the loss, this time of radicals of size x, due to all loss processes.

When chain termination occurs, "dead", non-free radical polymers, are produced, having degrees of polymerization equal to the sum of the degrees of polymerization of the free radicals that combined to produce them. These dead polymers can also nucleate the formation of liquid drops from the supersaturated monomer vapor (we assume that their quantitative effects in this respect are exactly the same as those of the corresponding free radicals of the same degree of polymerization), and so we must also consider the equations representing their rates of formation. If we denote by P_x the concentration of "dead" polymers of size x, then the typical equation for the rate of change of the concentration of dead polymers is

$$\frac{dP_x}{dt} = \left(\frac{k_t}{2}\sum_{i=1}^{i=x-1} R_{x-i}R_i\right) + k_{tr}MR_x - k_dP_x \tag{5}$$

The first expression in parentheses on the right of eq 5 sums the rates of all the bimolecular chain termination processes that can lead to the formation of a dead polymer of size x. Notice that the term $R_{x/2}R_{x/2}$, which occurs when x is even, is preceded by the factor $^1/_2$ as it should be, since otherwise this process would be counted twice. The second term on the right takes note of the fact that "dead" polymers of size x can also be produced by a chain transfer process involving a free radical of size x. Finally, the last term on the right of eq 5 accounts for the loss, through diffusion, of "dead" polymers of size x. We assume that the rate constant for this process is the same as for a *free radical* of the same size.

If we assume that a steady state is established in the reactions represented by eq 2, 4, and 5, the time derivatives on the left may be set to zero, and the equations may be solved for the various R_x and P_x, under the assumption that M remains constant (an extremely accurate assumption since M is present in enormous excess). The solution of eq 2 and 4 proceeds as follows. With the time derivatives set to zero and with θ assumed constant (in view of the steady state), simple inspection shows that R_x is given by the relation

$$R_x = \frac{k_iI + k_{tr}\theta}{k_p}\left[\frac{k_pM}{k_pM + k_{tr}M + k_t\theta + k_d}\right]^x \tag{6}$$

The quantity θ, defined by eq 3, is then a geometric series involving powers of the parameter in square brackets in eq 6. This series can be summed immediately to yield a quadratic equation for θ. When this quadratic is solved for θ and the result resubstituted into eq 6, we obtain for R_x

$$R_x = \left[\frac{k_iI}{k_p} + \frac{k_{tr}}{k_p}\left\{\frac{-k_d}{2k_t} + \left[\left(\frac{k_d}{2k_t}\right)^2 + \frac{k_iMI}{k_t}\right]^{1/2}\right\}\right] \times \left[k_pM \Big/ \left(k_pM + k_{tr}M + k_d + k_t\left\{\frac{-k_d}{2k_t} + \left[\left(\frac{k_d}{2kt}\right)^2 + \frac{k_iMI}{k_t}\right]^{1/2}\right\}\right)\right]^x \tag{7}$$

The solution of eq 5 is also simple. Because, according to eq 7, R_x involves the expression in the last brackets of eq 7 raised to the power x, the expression in parentheses on the right of eq 5 proves to be simply proportional to R_x. The solution of the resulting equation is then

$$P_x = \left[\frac{k_t}{k_pk_d}\left(\frac{x-1}{2}\right)\left[k_iI + k_{tr}\left\{\frac{-k_d}{2k_t} + \left[\left(\frac{k_d}{2k_t}\right)^2 + \frac{k_iMI}{k_t}\right]^{1/2}\right\}\right] + \frac{k_{tr}M}{k_d}\right]R_x \tag{8}$$

Since R_x is known from eq 7, P_x can be fully known from eq 8.

If chain transfer is not active, i.e., if $k_{tr} = 0$, then eq 7 and 8 become

$$R_x = \frac{k_iI}{k_p}\left[\frac{k_pM}{k_pM + \frac{k_d}{2} + k_t\left[\left(\frac{k_d}{2k_t}\right)^2 + \frac{k_iMI}{k_t}\right]^{1/2}}\right]^x \tag{9}$$

and

$$P_x = \frac{k_ik_tI}{k_pk_d}\left(\frac{x-1}{2}\right)R_x \tag{10}$$

From eq 9 we see that, if the intensity I becomes large enough, R_x may be approximated by

$$R_x = \frac{k_iI}{k_p}\left[\frac{k_pM}{(k_ik_tMI)^{1/2}}\right]^x \tag{11}$$

and if x is large, R_x becomes an inverse function of I. Thus, high enough values of light intensity reduce the steady-state concentration of large "live" polymers and, through the agency of eq 10, the concentrations of large "dead" polymers also. This is, of course, reasonable, since intense light will produce high concentrations of free radicals and thereby increase the chance of combinative chain termination. The effect is most marked with large polymers, since their production requires the successful completion of a large number of propagation steps. If the cloud chamber conditions are such that the polymer responsible for nucleation is large, we would, therefore, expect to see an eventual decrease in the rate of nucleation as the light intensity is increased.

In general, unless conditions are chosen to avoid the problem, nucleation will be due to nuclei having a variety of polymer compositions. As indicated in ref 1, the nucleation rate will depend on the frequency of encounters between polymers, the *sum* of whose molecular weights, or degrees of polymerization, add to the same sharply

critical value. These encounters can of course occur sequentially, so that some nuclei may contain a multiplicity of polymer molecules. We may denote each such nucleus composition by an index i. Then, invoking the law of mass action, we may denote the rate of nucleation, due to the ith process, by

$$J_i = K_i \prod_x R_x^{n_{xi}} \tag{12}$$

where K_i is an appropriate rate constant for the effective encounter rate between the polymer molecules involved in the nucleus and the index x runs over polymer sizes. The exponent n_{xi} represents the number of polymers of size x involved in the nucleus of the ith process. In eq 12, we only use the concentration of "live" polymers (denoted by R_x), under the assumption that both chain termination and transfer are moderate enough compared to propagation so that polymer molecules of each size are dominated by the "live" species. If this is not the case we can easily adjust the formula to include the effect of "dead" polymers. We note from eq 10 that the concentrations of "dead" polymers are at least proportional to those of the respective "live" ones but contain another factor of intensity I and also a linear dependence on degree of polymerization x. Furthermore, we note that when only *one* polymer molecule is involved in the nucleus, the quantity K_i is no longer an *encounter* rate since encounters between polymers will then be unnecessary. We return to this point later.

Now, as we have mentioned, the analysis in ref 1 indicates that the various nucleation processes (determined by the lifetime of a polymer before forming a drop) will be such that the summed monomeric content of all the polymers in the nucleus will approximate some constant that will depend upon the supersaturation. We may denote this constant by m and indicate the requirement by

$$\sum_{x=2}^{\infty} x n_{xi} = m \tag{13}$$

If we adopt eq 9 for R_x and define

$$\alpha = k_i I / k_p \tag{14}$$

and

$$\omega = \frac{k_p M}{k_p M + \frac{k_d}{2} + k_t \left[\left(\frac{k_d}{2k_t} \right)^2 + \frac{k_i M I}{k_t} \right]^{1/2}} \tag{15}$$

we have

$$R_x = \alpha \omega^x \tag{16}$$

Substituting eq 13 and 16 into eq 12 yields

$$J_i = (K_i \prod_x \alpha^{n_{xi}}) \omega^m \tag{17}$$

We also designate the number of polymer molecules involved in the ith nucleation process by

$$n_i = \sum_x n_{xi} \tag{18}$$

Then the total rate of nucleation may be expressed as

$$J = \sum_i J_i = (\sum_i K_i \alpha^{n_i}) \omega^m \tag{19}$$

Usually i in eq 19 will run over some possibly large, but finite number, N, of processes. Then through the following relation, we may define $\bar{K}$ and $\bar{n}$ as some sorts of average values of K_i and n_i:

$$\sum_i K_i \alpha^{n_i} = N \bar{K} \alpha^{\bar{n}} \tag{20}$$

Substituting this relation into eq 19 gives

$$J = N \bar{K} \alpha^{\bar{n}} \omega^m \tag{21}$$

It is clear that when a fewer number of processes are involved both $\bar{K}$ and $\bar{n}$ are more easily physically interpreted. In particular, when only one process is involved, $\bar{n}$ becomes the number of polymer molecules involved in the nucleus in that process (and as indicated previously, $\bar{K}$ is no longer an encounter rate). The ideal situation, and the one that should be established whenever possible in an experiment, is that in which only a single polymer molecule is involved in the nucleus. Then $\bar{n} = 1$, and, as we shall see below, m must be replaced by $m - 1$, where m represents the degree of polymerization of this single polymer.

Substituting eq 14 into eq 21 and taking the logarithm of both sides yields

$$\ln J = \ln N \bar{K} \left(\frac{k_i}{k_p} \right)^{\bar{n}} + \bar{n} \ln I + m \ln \omega \tag{22}$$

We write the equation in this form because we note from eq 15 that ω will be insensitive to intensity I when the I is low enough. At higher intensities, however, ω will be less than unity, and the last term on the right of eq 22 will be negative. This will cause the plot of $\ln J$ vs. $\ln I$, and, therefore, of J vs. I, to exhibit a maximum that represents the influence of chain termination.

At low light intensities, a plot of $\ln J$ vs. $\ln I$ should be linear with a slope equal to $\bar{n}$, the "average" number of polymer molecules involved in the nucleus. When only one nucleation process occurs, and that involves only *one* polymer molecule, the slope should be unity. Therefore, the occurrence of a unit slope implies that conditions have been achieved such that only *one* process, and only *one* polymer molecule, is involved.

Suppose that it has been ascertained, in this manner, that only one polymer molecule is involved. We might then use the theory of ref 1 (or, a more accurate theory—yet to be developed) to determine the degree of polymerization m of that polymer. Then, since the first term on the right of eq 22 (the intercept) and the slope $\bar{n}$ are known, the only unknown quantity is ω itself. We can then hope to determine ω by considering J at higher light intensities. However, in doing this, we must also be able to maintain that intensity low enough so that polymer molecules cannot encounter one another and engage in processes in which the nucleus contains more than one of them.

As indicated above, in the case where only one polymer molecule is involved, $\bar{K}$ no longer involves an *encounter* rate, and we elaborate this point now. In this case, the rate of nucleation is simply the rate of appearance of polymer molecules of the critical size, since every such molecule nucleates a drop immediately upon its arrival. If the critical degree of polymerization is m, then the rate of arrival of polymer of this size is given by the first term on the right of eq 4. Then eq 12 is replaced by

$$J = k_p M R_{m-1} = k_p M \alpha \omega^{m-1} = k_i M I \omega^{m-1} \tag{23}$$

and we may write

$$\ln J = \ln k_i M + \ln I + (m - 1) \ln \omega \tag{24}$$

which differs from eq 22 in having $\ln \omega$ preceded by $m - 1$ rather than m. We can of course still evaluate m from theory and so evaluate ω.

In the case of very low light intensity eq 24 can be expressed in the following manner. We first approximate ω, given by eq 15, as

$$\omega = k_p M/(k_p M + k_d) \quad (25)$$

by ignoring the quantity $k_i MI/k_t$ in comparison with the remaining quantities in brackets in the denominator on the right of eq 15. In the experiments, discussed in section IV, we have measured light intensity relative to a reference intensity, I_0. The actual light intensity, I, may then be expressed as

$$I = I_0 I_r \quad (26)$$

where I_r is the relative intensity. Then, using eq 26 and substituting eq 25 in eq 24 and rearranging we get

$$\ln J = \ln (k_i M) I_0 \left[1 + \frac{k_d}{k_p M} \right]^{-(m-1)} + \ln I_r \quad (27)$$

Thus as discussed above, at low light intensity and under conditions such that only one polymer of size m causes nucleation, the plot of $\ln J$ vs. $\ln I_r$ is a straight line with slope equal to unity. The intercept, however, is fairly complicated.

For low light intensity, the equation for the rate of nucleation involving more than one polymer also has a relatively simple form. The case in which the nucleus involves two polymers can be discussed in some detail. Again we substitute ω from eq 25 in eq 21 and take $\bar{n} = 2$. This gives

$$J = N\bar{K} \left(\frac{k_i I_0 I_r}{k_p} \right)^2 \left(\frac{k_p M}{k_p M + k_d} \right)^m \quad (28)$$

where eq 26 has been used. Now taking the logarithm of both sides

$$\ln J = \ln \left\{ N\bar{K} \left(\frac{k_i I_0}{k_p} \right)^2 \left(\frac{k_p M}{k_p M + k_d} \right)^m \right\} + 2 \ln I_r \quad (29)$$

Thus, a plot of $\ln J$ vs. $\ln I_r$ should again be a straight line, this time with slope equal to 2. Now the intercept contains, in addition to k_i, k_p, k_d, and m, the two additional quantities N and $\bar{K}$. N represents the number of pairs of polymer sizes that sum to m. Therefore, N should have a value of $m/2$ or $(m-1)/2$, depending on whether m is even or odd. $\bar{K}$ is, in fact, the binary collision frequency of these polymers and can be easily approximated with the help of gas kinetic theory.

As mentioned earlier, eq 22 indicates that at low light intensities, plots of $\ln J$ vs. $\ln I_r$ should be straight lines with slopes equal to $\bar{n}$, where $\bar{n}$ is the average number of polymers involved in each nucleus. However, a quantitative analysis of the intercepts for $\bar{n} > 2$ is extremely difficult.

Returning to eq 23, we see that the quantity $k_i MI/k_t$ in eq 15 cannot, in general, be ignored. For example, it cannot be neglected when the light intensity is moderate or high. However, substituting for ω from eq 15 and rearranging, we get

$$\frac{J}{I_r} = k_i I_0 M \left(1 + \frac{k_d}{2k_p M} \right)^{1-m} \left[1 + \left(\frac{4k_i k_t MI_0 I_r}{2k_p M + k_d} \right)^{1/2} \right]^{1-m} \quad (30)$$

where it has been assumed that $(k_d/2k_t)^2$ is negligible in comparison with $k_i MI/k_t$. Now, at not too high values of I_0, $[4k_i k_t MI_0 I_r/(2k_p M + k_d)]^{1/2}$ can be assumed to be much less than unity, and therefore, expanding the expression in brackets in eq 30 gives, after rearrangement,

$$\frac{J}{I_r} = k_i MI_0 \left(1 + \frac{k_d}{2k_p M} \right)^{1-m} - (m-1) \left(1 + \frac{k_d}{2k_p M} \right)^{-m} \left[\frac{k_i^3 k_t MI_0^3}{k_p^2} \right]^{1/2} I_r^{1/2} \quad (31)$$

We see that a plot of J/I_r vs. $I_r^{1/2}$ should be a straight line with a negative slope.

We, now have at hand a number of expressions for the slopes and intercepts of the various plots. But inspection reveals that these expressions are very complicated, involving high powers of combinations of several rate constants. Furthermore, the number of unknowns exceeds the number of equations available from our present experiments. In principle, however, further relationships can be obtained from the study of non-steady-state processes in the cloud chamber.

Table I
Values of Supersaturation, Temperature, and Partial Pressure of Vinyl Acetate at an Elevation of 0.73 (Level of the UV Beam) in the Cloud Chamber

S	T, K	P, torr
2.58	270.7	67.4
2.32	271.4	63.3
1.94	286.3	118.4
1.69	283.2	88.2
1.57	279.4	66.8

IV. Results and Discussion

In this section we present and discuss our experimental data, together with analysis in terms of the theory presented in the preceding section.

As will be clear, the polymers responsible for the nucleation process have degrees of polymerization of the order of 50, and, in future experiments, involving higher precision and performed at much lower supersaturations, we should be able to investigate even larger ones. Even a polymer having a degree of polymerization of 50, however, is probably substantially larger than any of those previously investigated "reliably" in the vapor phase.[7]

As indicated in section III, in our experiments it has proved convenient to measure light intensity I_r relative to a reference level I_0. In the equations of section III, I_r was properly included, by replacing I, wherever it appeared, by $I_r I_0$. Figure 4 exhibits the observed dependences, on I_r, of the rates of nucleation[23] of vinyl acetate vapor, by its polymers, at five values of supersaturation of the vapor. The values of supersaturation, temperature, and partial pressure of vinyl acetate (listed in Table I), corresponding to the level of the UV beam in the chamber, have been calculated by iteratively solving the heat and mass flux equations[9,10] for the chamber. In our experiments, boundary temperatures (surface of *pool* on the plate, and *film* on the upper plate) used for this purpose are somewhat imprecise (~2 °C) because the thermocouples employed for measuring them were not located at the respective surfaces but, rather, embedded in the metal plates themselves. As a result our supersaturations could have inaccuracies as large as 10%. This situation resulted from the necessity to use a chamber designed originally for another purpose. However, it should be emphasized that the uncertainty in supersaturation has *no* effect on almost *every* aspect of the current investigation, the one exception being the estimate of the activation energy for propagation, which is performed with the help of Figure 8, where an

error of about 7% is introduced.

Care was taken to ensure that the highest supersaturation employed in the experiments remained lower than that in which homogeneous nucleation occurred, so that we could be sure that the observed nucleation was always photoinduced, and, most likely, by poly(vinyl acetate). At all levels of supersaturation at which kinetic studies were performed, no "dark" nucleation was observed, and at least 30 s elapsed between the time at which the UV lamp was switched on and the onset of nucleation.

At high rates of nucleation, the counter readings had to be corrected to account for coincidences when more than one droplet fell through the laser beam at the same instant of time, creating only a single pulse. The correction was made, using a theory due to Flageollet-Daniel et al.[19]

It is convenient to discuss the analysis of our data as six separate items. These involve agreement between theory and experiment, as well as among themselves, which is variously quantitative, semiquantitative, and qualitative. However, in view of the "bootstrap" nature of our investigation, all pieces of information are important. The six items are as follows:

(1) The dependence of ω on light intensity, exhibited in eq 15 requires, when substituted into eq 22, the plot of J vs. I to pass through a maximum. Furthermore, the maximum should occur at higher values of I if the polymers responsible for the nucleation process are smaller. This maximum, which is a result of the chain termination process, is actually observed in the experimental data, and the dependence of its location on polymer molecular weight is consistent with the theory. The plots in Figure 4 show that (as indicated by eq 22) at high degrees of supersaturation, e.g., 2.58 and 2.32 (measured by *our* thermocouples), the rate of nucleation increases with increasing light intensity, reaches a maximum, and then decreases with further increase in intensity. According to the theory of section III, the value of light intensity at which this maximum occurs depends (as shown below) on, besides the various rate constants, the size of the polymers causing nucleation. We have seen, in section III, that either a single polymer of a certain size, m, or an average number of polymers, each of average size $m/\bar{n}$, can be responsible for nucleation at different levels of supersaturation. Now, when only one polymer is involved in the nucleus, the maximum in J actually corresponds to the maximum in the concentration R_m. In order to find an expression for this maximum, we make use of the expression for R_m given by eq 9, setting the derivative of R_m (with respect to I_r) equal to zero. If, in this process, we neglect $(k_d/2k_t)^2$ in comparison with (k_iMI/k_t) in eq 9, it is easy to show that the value of relative intensity at the maximum is

$$I_r^* = \frac{4k_p^2M(1 + k_d/2k_pM)^2}{k_ik_tI_0(m - 2)^2} \qquad (32)$$

This equation indicates that I_r^* depends inversely on m, the size of the polymer. Therefore, the position of the maximum in the plot of J vs. I_r will shift toward higher values of I_r as smaller polymers are involved in the nucleus. This prediction is supported by our experimental data. We see that, at $S = 2.58$ (where S denotes supersaturation), and, as we shall see later only one polymer is involved in causing nucleation, the maximum occurs at $I_r^* = 0.6$. At the lower supersaturation, $S = 2.32$, and, as we shall see later, two polymers of smaller average size are responsible for nucleation. The concentrations, R_x and R_{m-x}, for each of these polymers must each show a maximum at higher values of I_r^* than the value at which the maximum occurs for the concentration of the single polymer, effective at S = 2.58. Since there is no significant change in M and temperature at these two supersaturations (see Table I), k_i, k_p, k_t, and k_d are likely to remain unchanged in eq 32. Therefore I_r^* at $S = 2.32$ should increase, and, in Figure 4, we, indeed, find $I_r^* = 0.8$. At still lower supersaturations, e.g., 1.94, 1.69, and 1.57, greater numbers of polymers are involved in each nucleus, and these are most likely to be still smaller. Consequently I_r^* should be still greater. In fact, in these latter cases, I_r^* values lie beyond the range of relative light intensities (bounded by $I_r = 1.0$) investigated by us. As a consequence we do not observe any maximum in any of these plots.

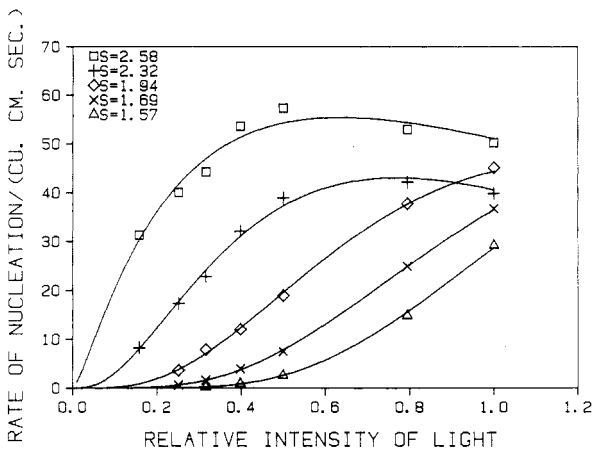

Figure 4. Plots of the rate of nucleation vs. relative light intensity at various supersaturations and temperatures of vinyl acetate. Elevation of the He–Ne laser beam = 0.52; reference light intensity $I_0 = 1.8 \times 10^{15}$ photons cm^{-2} s^{-1}.

Although we report a supersaturation of 2.58 for the highest curve in Figure 4, the uncertainty arising from the above-mentioned positioning of the thermocouples allows one to only bound this supersaturation between 2.3 and 2.6, although probably closer to 2.3. Corresponding to this range, and according to Table II of ref 1, the degree of polymerization of the single polymer molecule responsible for nucleation should lie in the range between 35 and 50, but closer to 50.

(2) Another observation, and one that tends to confirm that the observed nucleation is due to poly(vinyl acetate) molecules, rather than another, nongrowing polymeric free radical, is the occurrence of abundant nucleation in regions of lower supersaturation outside of the UV beam.

In the case of ordinary photoinduced nucleation, e.g., as with the photooxidation of SO_2 (see ref 12), the species responsible for the nucleation may diffuse out of the UV beam to regions, in the cloud chamber, of lower supersaturation, but is not usually effective in inducing nucleation in these regions, since it is barely able (under the experimental conditions) to cause nucleation in the region of higher supersaturation through which the light beam passes. In contrast, in the case of growing polymer radicals, escape by diffusion does not imply that the radical stops growing. Hence it may continue to grow until it becomes large enough to cause nucleation in a region of lower supersaturation. This phenomenon has been observed in the present experiment.

For example, it was observed that if the He–Ne laser beam, used for detection, was lowered so as to increase the volume of observation above the laser beam, the measured rate of nucleation was higher. This is illustrated in Figure 5. The plots in Figure 5 therefore indicate that abundant nucleation occurs at locations outside the region of maximum supersaturation at which the UV beam is aimed. This shows that free radical chains that escape the regions

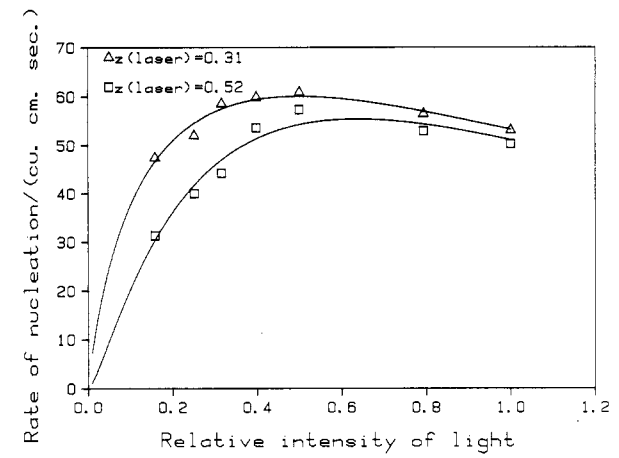

Figure 5. Plots of rate of nucleation against relative light intensity for various elevations (z_{laser}) of the He–Ne laser beam. $S = 2.58$, $T = 270.7$ K, and $I_0 = 1.8 \times 10^{15}$ photons cm^{-2} s^{-1}.

Table II
Values of the Slopes and the Intercepts of the Plots log J vs. log I_r at Various Supersaturations

S	slope	intercept
2.58	1.15	2.34
2.32	2.03	2.50
1.94	3.56	2.70
1.69	4.95	2.67
1.57	7.18	2.80

by diffusion do indeed continue to grow until they are large enough to act as nuclei at lower supersaturations. In the case of photoinduced nucleation, not involving polymer free radicals, such additional nucleation is not likely when the light intensity is just sufficient to cause nucleation at the maximum supersaturation. It should be noted that the data in Figure 4 were obtained by positioning the He–Ne laser beam at the highest practical elevation, below the UV beam, so that, as much as possible, measurement of additional nucleation outside the beam could be eliminated.

(3) We are able to show that at a sufficiently high degree of supersaturation, together with a low enough light intensity, conditions are established under which the process of nucleation is dominated by nuclei in which only *one* polymer molecule is involved. In terms of eq 27 this means that, in plots of our data, the logarithm of the nucleation rate appears as a linear function, with unit slope, of the logarithm of light intensity.

We now plot our data as log J vs. log I_r. According to the theory of section III, and especially to eq 22 and 27, such plots should be straight lines with slopes equal to the number of polymer molecules involved in the nucleation process. In Figure 6 our data have been plotted in this way (at very low values of I_r ($I_r < 0.3$)), for the various levels of supersaturation at which measurements were performed. Indeed, these plots are fairly good straight lines. Table II lists the observed values of the slopes and intercepts of these lines. The slope of the curve for $S = 2.58$ (our measurement of supersaturation; as explained earlier, the true value is probably closer to 2.3) is unity, within experimental error. Equation 27, therefore, implies that, at this supersaturation, the critical nucleus contains only *one* polymer molecule. Thus, we have apparently been able to achieve the desired situation in which only one polymer is involved in the nucleus. The slope of the curve in Figure 6 corresponding to $S = 2.32$ (our measurement) is approximately 2, and this implies that two molecules are active in the nucleus. The successive plots for $S = 1.94$, 1.69, and 1.57 (our measurements) correspond to 3.56, 4.95,

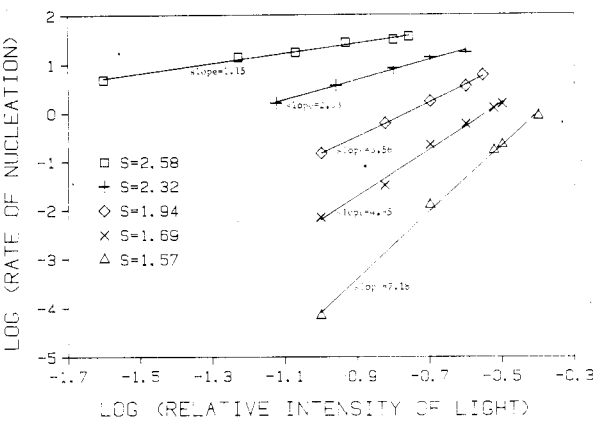

Figure 6. Plots of logarithm of rate of nucleation against logarithm of relative light intensity at various supersaturations. Elevation of the He–Ne laser beam = 0.52; $I_0 = 1.8 \times 10^{15}$ photons cm^{-2} s^{-1}.

and 7.18 molecules in the nucleus, respectively. We note that greater numbers of polymer molecules are required in the nucleus as the supersaturation is lowered. This is fully in accord with the expectations of theory.

There is, however, one point that needs to be resolved. All the plots in Figure 6 are in the range of low light intensity. Nevertheless, in this range, processes corresponding to several polymer molecules in the nucleus seem to be active. Reference to Figure 4, which is not a log–log plot, and therefore easier to interpret quantitatively, reveals that the rates at the lower supersaturations are already nonzero in this range, although they are considerably smaller than that for the one-polymer process. Thus, in Figure 4 the curve corresponding to what is apparently a *two*-polymer process is, at $I_r = 0.3$, almost 0.7 times as large as that for the one-polymer curve at $S = 2.58$. If, at a given intensity, the supersaturation is increased, the nominal concentration of polymers remains unchanged, since it is controlled, essentially, by the light intensity. If a two-polymer process is already active, at a given intensity at $S = 2.32$, it will be even more active at $S = 2.58$. Therefore, the two-polymer process should certainly compete with the one-polymer mechanism at the higher supersaturation, if it is already occurring at the lower one. Then it becomes necessary to explain how the approximately unit slope of a curve corresponding to $S = 2.58$ in Figure 6 comes into being. In fact, a satisfactory explanation can be given as follows.

For simplicity, we only consider the effect on the one-polymer curve ($S = 2.58$) of the two-polymer process ($S = 2.32$). We confine attention to the range I_r extending up to $I_r = 0.3$. In accordance with eq 23 and 28, we have

$$J = k_i M I_0 I_r \omega^{m-1} + N\bar{K}\left(\frac{k_i I_0 I_r}{k_p}\right)^2 \omega^m \qquad (33)$$

From Figure 4, we see that at $I_r \approx 0.5$ the contribution due to the two-polymer process is approximately equal to that of the one-polymer process. Thus we may write

$$k_i M I_0 \omega^{m-1}(0.5) = N\bar{K}\left(\frac{k_i I_0}{k_p}\right)^2 \omega^m (0.5)^2 \qquad (34)$$

which may be rearranged to yield

$$N\bar{K}\left(\frac{k_i I_0}{k_p}\right)^2 \omega^m = 2 k_i M I_0 \omega^{m-1} \qquad (35)$$

Substituting eq 35 into eq 33 gives

$$J = k_i M I_0 \omega^{m-1}(I_r + 2I_r^2) \qquad (36)$$

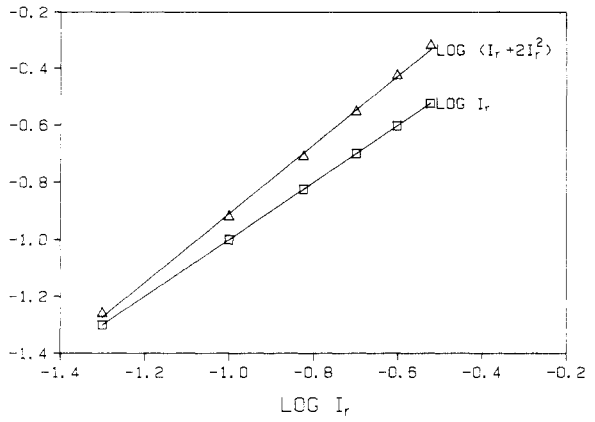

Figure 7. Plots of log I_r and log $(I_r + 2I_r^2)$ vs. log I_r.

This equation reduces to eq 27 if we neglect $2I_r^2$ in comparison with I_r and take the logarithm of both sides as well as make proper substitutions.

It is possible to almost ignore $2I_r^2$ when I_r is small. This point is made most effectively by ref to Figure 7, in which we show plots of log $(I_r + 2I_r^2)$ and log I_r vs. log I_r in the range of intensities covered by Figure 6. The plot of log I_r is obviously a straight line with a slope of 1.0. However, the plot of log $(I_r + 2I_r^2)$ is, also, almost a straight line with a slope of 1.21. In fact, this slope is almost identical with the slope of the curve in Figure 6, corresponding to S = 2.58 (our measurement).

Thus we can justify the apparent linearity of the curves in Figure 6 even though, as in the case of the one at S = 2.58, we know that, except at very very low light intensity, there must be some contribution from processes involving more than one polymer molecule. It is the process involving the smallest number of polymer molecules that dominates the shape of the curve.

(4) We do not, at this stage, have enough precise data to be able to unfold, from the various slopes and intercepts, all of the kinetic parameters involved in the mechanism. When reliable values of supersaturation are obtained, in the future, it should be possible to use information from the theory of nucleation, developed in ref 1, to obtain values for these parameters. However, even at this stage, we can make some estimates in order to demonstrate the "order of magnitude" consistency of theory and experiment. The following example elaborates this point.

From the intercept of the linear plot mentioned in item 3, together with a value of m estimated from the supersaturation and Table II of ref 1, it is possible to estimate the activation energy in the propagation constant, k_p. The value for the activation energy obtained in this manner is consistent with the value obtained from rate studies of bulk polymerization.[20] We proceed by referring to Figure 6.

In this figure, the intercept of the curve corresponding to S = 2.58 is 2.34 (see Table II). Therefore, applying eq 27, we have

$$k_p = \frac{k_d}{M}\left\{\left(\frac{k_i M I_0}{10^{2.34}}\right)^{1/(m-1)} - 1\right\}^{-1} \tag{37}$$

We may express k_p in the form

$$k_p = Zfe^{-E_p/RT} \tag{38}$$

where Z is the (kinetic theory) collision number, f, the steric factor, and E_p, the activation energy while R is the gas constant. Substituting eq 38 into eq 37 and rearranging the latter yield

$$E_p = RT \ln \frac{ZfM}{k_d} + RT \ln \left\{\left(\frac{k_i M I_0}{10^{2.34}}\right)^{1/(m-1)} - 1\right\} \tag{39}$$

We can use eq 39 in the following manner. Reasonable estimates are available for all of the parameters appearing on the right of the equation, and we can specify a *range* of possible values for m using Table II of ref 1 and the measured value of supersaturation. However, as we have indicated previously, the most that we are able to say about S at this time is that it lies in the range 2.3–2.6, and probably closer to 2.3. This means, according to Table II of ref 1, that m lies in the range 50–35, but probably closer to 50. Therefore, we shall employ our best estimates of the other parameters in eq 39 and use the equation to plot E_p as a function of m in a range including m = 35–50. Hopefully, this value of E_p will be reasonably consistent with values measured by other means. The value measured for bulk polymerization[20] is about 4000 cal mol^{-1}, while Melville et al.[5] report an approximate value for the gas-phase process of 1400 cal mol^{-1}. The latter value is for a vinyl acetate pressure below 40 torr and is unfolded from a complicated, somewhat speculative formula. Since measurements on gas-phase polymerization have to be used cautiously (see earlier comments), we must place less weight on this lower value of E_p. The most unbiased procedure involves letting the "chips fall where they may", in respect to eq 39, and allowing the value of E_p to evolve as the equation requires.

The constant k_i is equal to the product of the extinction coefficient and quantum efficiency involved in the generation of the initiating free radical. The value of the extinction coefficient, ϵ, is very sensitive to trace impurities that may be present in vinyl acetate, and Matheson et al.[21] have reported a value of 0.1 L mol^{-1} cm^{-1} for their sample in the wavelength region between 260 and 280 nm. The quantum yield[22] ϕ has been determined to be 0.3 for vinyl acetate at 254 nm. These results lead to a value of

$$k_i = 5 \times 10^{-23} \text{ cm}^3 \text{ molecule}^{-1} \text{ cm}^{-1} \tag{40}$$

M, the monomer concentration, is obtained from Table I as

$$M = 2 \times 10^{18} \text{ cm}^{-3} \tag{41}$$

while I_0, the reference intensity, as measured by the power meter, is equal to

$$1.8 \times 10^{15} \text{ photons cm}^{-2} \text{ s}^{-1} \tag{42}$$

Z and f are estimated as follows. The steric factor should be less in the gas than in bulk polymerization.[20] A monomer striking a growing polymer in the vapor must find its way to the free radical "head" of the polymer. We therefore choose f to be 0.05 of its value in bulk, i.e., $f = 5 \times 10^{-7}$, since the reported[20] bulk polymerization value is 10^{-5}. The collision number Z is available from the standard formula of gas kinetic theory. The vinyl acetate parameters required for this formula are the collision radius for the reaction and the mass of the vinyl acetate molecule. We take, as nominal values of these quantities, 10^{-7} cm for the collision radius and 1.45×10^{-22} g for the molecular mass. Then the collision number at 271 K is

$$Z = 8.1 \times 10^{-10} \text{ cm}^3 \text{ molecule}^{-1} \text{ s}^{-1} \tag{43}$$

Next, we need the rate constant corresponding to the diffusive escape of radicals from the UV beam. In estimating k_d we follow a procedure described in a paper by Marvin and Reiss,[12] assuming the same geometry. First, the binary diffusion coefficient of the polymers through

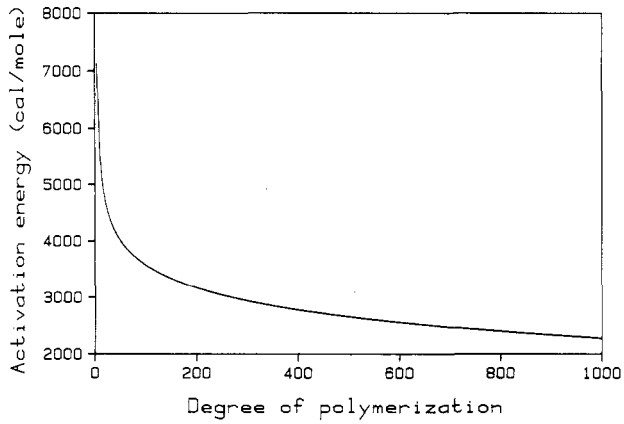

Figure 8. Plot of activation energy for propagation E_p against degree of polymerization m of the polymers causing nucleation.

helium is estimated from the standard kinetic theory formula

$$D = \frac{\left[\frac{2kT}{\pi}\left(\frac{1}{m_1} + \frac{1}{m_2}\right)\right]^{1/2}}{\pi(r_1 + r_2)^2(n_1 + n_2)} \tag{44}$$

Here, k is the Boltzmann constant, m_1 is the mass of the helium atom = 6.6×10^{-24} g, m_2 is the mass of a polymer molecule, 2×10^{-21} g, r_1 is the collision radius of the helium atom, 1.1×10^{-8} cm, r_2 is the collision radius of a polymer molecule, 10^{-7} cm, n_1 is the concentration of helium molecules, 2.4×10^{19} cm^{-3}, and n_2 is the concentration of polymer molecules, 2×10^{11} cm^{-3}. From eq 44 we therefore find $D = 0.07$ cm^2 s^{-1}. By using the methods of section VIII of ref 12 we find

$$k_d = \frac{2\pi r_0 D(\partial c/\partial r)_{r=r_0}}{\pi r_0^2 c(r_0)} = \frac{2D}{r_0^2 \ln (R_0/r_0)} \tag{45}$$

In the cloud chamber employed in these experiments we have r_0, the radius of the UV beam, equal to 0.6 cm, and R_0, the radius of the "cylindrical" space between the center of the UV beam and the plates, approximately 2.9 cm. These are, of course, only nominal values. However, substituting D, r_0, and R_0 into eq 45 we find

$$k_d = 0.245 \text{ s}^{-1} \tag{46}$$

We now have all the parameters necessary for substitution in eq 39, and we can use that equation to plot E_p vs. m. Such a plot appears in Figure 8, and we note that the values of E_p in the range of m lying between 35 and 50 (the range corresponding to the supersaturation in the chamber) is narrowly confined to the neighborhood of 4000 cal mol^{-1}. Since the nominal value measured for E_p in the process of bulk polymerization is 4000 cal mol^{-1}, our results are in the range of independent measurements even to this detail.

(5) The conclusions concerning E_p allow another demonstration of the validity of the overall mechanism. Coupled with the values of Z and f, prescribed above, this leads to the following value at 271 K of k_p (see eq 38):

$$k_p = 2.408 \times 10^{-19} \text{ cm}^3 \text{ molecule}^{-1} \text{ s}^{-1} \tag{47}$$

The value of k_d in eq 46 and M prescribed by eq 41 then allow us, according to eq 25, to calculate ω at low intensities

$$\omega = k_p M/(k_p M + k_d) = 0.663 \tag{48}$$

Furthermore, employing the value of α (appropriate to low light intensity) in eq 14, using k_i from eq 40 and I_0 from eq 42, and setting $I_r = 0.05$, we find

$$\alpha = 1.8 \times 10^{10} \text{ photons cm}^{-3} \tag{49}$$

Consider, now, binary encounters between two polymers, the sum of whose degrees of polymerizations is always m'. The rate of *all* of these processes is thus

$$J_2(m') = \sum_{x=1}^{m'-1} Z(x)R_x R_{m-x} = \left(\frac{m'-1}{2}\right)\bar{Z}(m')\alpha^2\omega^{m'} \tag{50}$$

where $Z(x)$ is the collision number for an encounter between polymers of size x and $m - x$, $\bar{Z}(m')$ is some appropriate "average" collision number for encounters "summing" to m', and we have used eq 16. The rates of nucleation due to *all* binary encounters include all for which m' exceeds the critical value m, i.e.

$$J_2 = \sum_{m'=m}^{\infty} J_2(m') = \frac{\tilde{Z}\alpha^2}{2}\left\{\left(\frac{m-1}{1-\omega}\right)\omega^m + \frac{\omega^{m+1}}{(1-\omega)^2}\right\} \tag{51}$$

where $\tilde{Z}$ is an "average" Z for all values of m'. $\tilde{Z}$ and $\bar{Z}$ can certainly be accurately estimated by $Z(m/2)$. With little loss of precision we then have

$$J_2 \approx Z(m/2)\frac{\alpha^2}{2}\left\{\left(\frac{m-1}{1-\omega}\right)\omega^m + \frac{\omega^{m+1}}{(1-\omega)^2}\right\} \tag{52}$$

In order to evaluate $Z(m/2)$ we require the collision radius for an "average"-sized polymer (involved in the encounter). If we assume this to be a polymer with $x = 40$, i.e., $m \approx 80$, and compute its volume as 40 times the volume per molecule in the monomer liquid, we calculate a radius of 1.2×10^{-7} cm and a collision radius of 2.4×10^{-7} cm. The reduced mass of the collision is 2.86×10^{-21} g. Substitution of these numbers into the standard kinetic theory formula gives, at 271 K,

$$Z(m/2) = 4.2 \times 10^{-8} \text{ cm}^3 \text{ molecule}^{-1} \text{ s}^{-1} \tag{53}$$

When eq 48, 49, and 53 are substituted into eq 52 with $m = 80$, we obtain

$$J_2 \approx 8.5 \text{ cm}^{-3} \text{ s}^{-1} \tag{54}$$

Now refer to Figure 4. We note that the curve for $S = 2.32$, which we now believe to represent nucleation involving a nucleus containing two polymer molecules, gives a J of the same order as eq 54 at $I_r = 0.05$ (the experimental value, obtained by extrapolation, is 0.8). More important the two-polymer curve is just beginning to show an active rate at $I_r = 0.05$, and the same is true of the estimate in eq 52. Thus the result is consistent if we assume for the curve marked by the supersaturation 2.32, $m = 80$.

(6) The linear character of a plot of ln J vs. ln I, at low light intensities, is, of course, inappropriate at higher light intensities. However, when only one polymer molecule is involved in the nucleus, a plot of J/I_r vs. $I_r^{1/2}$ should, according to theory, be a straight line with negative slope. Even this feature appears in our experimental data.

If only one polymer molecule is involved in the nucleus, we should be able to apply eq 31 across the entire range of measured relative intensities. This equation predicts that, when only one polymer molecule is involved, a plot of J/I_r vs. $I_r^{1/2}$ should be a straight line with a negative slope. With this in mind we accumulated data for a level of supersaturation of 2.58 (our measurement) using two different reference intensities I_0. According to our previous discussion, at $S = 2.58$, only one molecule should be in-

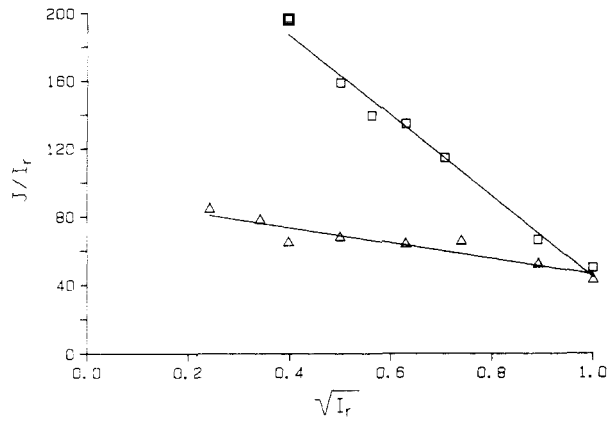

Figure 9. Plots of J/I_r against $I_r^{1/2}$ at two reference intensities. $S = 2.58$, $T = 270.7$ K, and elevation of the He–Ne laser beam = 0.52.

Table III
Data Obtained from the Plots of J/I_r vs. $I_r^{1/2}$

$I_0 \times 10^{-15}$, photons cm^{-2} s^{-1}	slope, cm^{-3} s^{-1}	intercept, cm^{-3} s^{-1}	ratio of intercepts	ratio of slopes
1.8	−237.9	282.6		
0.6[a]	−46.0	92.4	3.1	5.2

[a] This value has not been measured but has been calculated from the ratio of the intercepts.

volved in the nucleus. In Figure 9 we have plotted these two sets of data as J/I_r vs. $I_r^{1/2}$. The slopes and intercepts of these plots are listed in Table III. At very high light intensities we should expect deviation from linearity due to the increasingly significant contribution of multipolymer nucleation processes. However, no such deviation is observable in the plots of Figure 9. On the contrary these plots confirm eq 31 and the assumed kinetic mechanism upon which it is based.

Without entering into detailed quantitative analysis of the slopes and intercepts of these plots, we can make the following point. The ratio of the intercepts of the two plots is equal to 3.1, indicating, according to eq 31, that the ratio of the reference intensities is 3.1. Then, also according to eq 31, the ratio of the slopes of the two plots should be $(3.1)^{3/2}$ or 5.5. Table III shows that the experimental ratio of slopes is 5.2, in agreement with this value, within experimental error. Thus, our data confirm, in a rather dramatic way, the detailed, assumed mechanism and indicate that, especially at high light intensities, chain termination by radical combination plays a significant role in the polymerization process.

In conclusion we believe that the applicability of this new method for the study of gas-phase polymerization kinetics has been demonstrated. The combination of nucleation theory, as developed in ref 1, and the chemical kinetic theory developed in section III of the present paper leads to predictions that are confirmed, by experiment, and that exhibit internal consistency.

We have been able to accumulate compelling evidence that the observed photonucleation is indeed due to the formation of polymers. In this connection we note the occurrence of additional nucleation in regions of lower supersaturation outside of the UV beam, the occurrence of maxima in the plots of nucleation rate vs. light intensity (an indication of chain termination by bimolecular combination of free radicals), and the demonstration of an activation energy consistent with that measured for propagation in a bulk system. Furthermore, the shapes of various plots involving nucleation rate and light intensity confirm, in both quantitative and qualitative detail, the predictions of section III. For example, at low light intensities, log–log plots involving nucleation rate and intensity are straight lines with slopes ranging from the order of unity to much higher values. Those, of order unity, are expected when the nucleus for condensation involves only one polymer molecule. We have therefore been able to present evidence that it is possible to establish cloud chamber conditions such that only *one polymer molecule* is active in this respect (a situation that is particularly suited to chemical kinetic studies). We have also been able to show that the observed relative intensity at which processes involving nuclei having two polymers become active is consistent with all the other features of the assumed mechanism. In addition, plots of J/I_r when plotted, for the "one-molecule" curve, vs. $I_r^{1/2}$ are straight lines across the entire range of light intensities that we employed. This behavior is predicted by the theory of section III, when only one molecule is involved in the nucleus, and the chain termination process involves bimolecular free radical combination. Curves obtained with reference light intensities of different magnitude are also consistent with respect to one another within the bounds of the theory.

Finally the degrees of polymerization that are being sensed by our method are of the order of 50, and, even in this first attempt these molecules are certainly considerably larger than any others upon which truly quantitative studies in the gas phase have been performed heretofore.

We are now in a position to perform future experiments with an experimental system designed to eliminate any sources of imprecision inherent in the apparatus used in the present work. This includes both the cloud chamber and the various optical and electronic systems. In future experiments, by moving to much lower supersaturations and much lower count rates, we should be able to perform experiments with even larger polymers. For example, Table II of ref 1 indicates that, at supersaturations as low as 1.35, we should be able to observe degrees of polymerization as large as 1000. It may even be possible to go higher.

Finally, we remark on an interesting feature of the present experiment. This concerns the fact that the observed rate of nucleation is really the observed rate of reaction (i.e., the observed rate of arrival of a polymer of a given size). The fluctuations that are observed in the rate of nucleation are therefore fluctuations in the rate of chemical reaction. We are therefore actually observing the "noise" in the *chemical reaction* itself. This feature is a result of the extremely small rate of reaction under observation, amounting to only a few molecular conversions per cubic centimeter per second.

Acknowledgment. This work was supported by Grant No. ATM8213871 from the Army Research Office at Durham and NSF Grant No. H820801.

Registry No. Vinyl acetate, 108-05-4.

References and Notes

(1) H. Reiss and M. A. Chowdhury, *J. Phys. Chem.*, **87**, 4599 (1983).
(2) G. Odian, "Principles of Polymerization", McGraw-Hill, New York, 1970, pp 172–175.
(3) H. W. Melville, *Proc. R. Soc. London, Ser. A*, **163**, 511 (1937); **167**, 99 (1938).
(4) C. H. Bamford and M. J. S. Dewar, *Proc. R. Soc. London, Ser. A*, **197**, 356 (1941).
(5) H. W. Melville and R. F. Tuckett, *J. Chem. Soc., Part 2*, 1201, 1211 (1947).
(6) J. Heicklen, *J. Am. Chem. Soc.*, **87**, 445 (1965).
(7) D. G. Marsh and J. Heicklen, *J. Am. Chem. Soc.*, **88**, 269 (1966).
(8) J. L. Katz and B. J. Ostermier, *J. Chem. Phys.*, **47**, 478 (1967).
(9) J. L. Katz, *J. Chem. Phys.* **52**, 4733 (1970).

(10) J. L. Katz, *J. Chem. Phys.*, **62**, 448 (1974).
(11) J. L. Katz, C. J. Scoppa II, N. G. Kumar, and P. Mirabel, *J. Chem. Phys.*, **62**, 448 (1975); J. L. Katz, P. Mirabel, C. J. Scoppa II, and T. L. Virkler, *ibid.*, **65**, 382 (1976).
(12) D. C. Marvin and H. Reiss, *J. Chem. Phys.*, **69**, 1897 (1978).
(13) A. W. Gertler, J. O. Berg, and M. A. El-Sayed, *Chem. Phys Lett.*, **57**, 343 (1978); A. W. Gertler, B. Almeida, M. A. El-Sayed, and H. Reiss, *Chem. Phys.*, **42**, 429 (1979).
(14) P. Mirabel and J. L. Clavelin, *J. Chem. Phys.*, **70**, 2048, 5767 (1979).
(15) B. Cordier, P. Papon, and J. Leblond, *J. Chem. Phys.*, **74**, 3353 (1981).
(16) F. C. Wen, T. McLaughlin, and J. L. Katz, *Phys. Rev. A*, **26**, 2235 (1982).
(17) G. Odian, "Principles of Polymerization", McGraw-Hill, New York, 1970, p 170.
(18) Reference 17, pp 203–212.
(19) C. Flageollet-Daniel, P. Ekrhard, and P. Mirabel, *J. Chem. Phys.*, **75**, 4615 (1981).
(20) H. W. Melville and G. M. Burnett, *Proc. R. Soc. London, Ser. A*, **189**, 456 (1947).
(21) M. S. Matheson, E. E. Auer, E. B. Evilaclua, and E. J. Hart, *J. Am. Chem. Soc.*, **71**, 2610 (1949).
(22) "Vinyl Polymerization", Vol. 1, Part I, G. E. Ham, Ed. Marcel Dekker, New York, 1967, p 293.
(23) The rates quoted in this section and in the various figures are actually the rates at which drops fell through the volume of observation in the laser beam. This rate is about half the rate of nucleation, J (cm^{-3} s^{-1}), in the UV beam. For the purposes of this discussion no error, whatsoever, is incurred by using these rates for J, except in eq 39, where it results in an almost negligible error, in E_p, of about 20 cal.

Pulsed Laser Spectroscopic Study of the Photoisomerization of Azo Labels at Three Different Locations on a Polystyrene Chain†

Chong Sook Paik Sung*

Department of Materials Science and Engineering, Massachusetts Institute of Technology, Cambridge, Massachusetts 02139

Ian R. Gould and Nicholas J. Turro

Department of Chemistry, Columbia University, New York, New York 10027.
Received December 29, 1983

ABSTRACT: Azobenzene chromophores have been incorporated as molecular labels at three specific sites on a polystyrene chain: the chain end, the chain center, or as the side group. Trans ⇄ cis photoisomerization kinetic behavior of azo labels has been studied both in dilute solution and in the glassy state at 20 °C, using nanosecond pulsed laser spectroscopy, which reduced the measurement time to only 2 s. In dilute solution, a small difference in the label's photoisomerization behavior has been observed at different sites of the chain; the end label can photoisomerize a little faster than the center label or the side label. A much greater difference is observed in the glassy state, especially between the end label and the center label, mainly due to the free volume differences in the vicinity of each label. Assuming that in the glassy state, only a certain fraction of the label can isomerize with the same rate as in dilute solution, only 8% of the center label is found to photoisomerize while about 45% of the chain end or the side group photoisomerizes at 20 °C. The experimental results are discussed in terms of the theoretical predictions based on the free volume size distribution theory of Robertson, which was applied to meet the photoisomerization requirement of the azobenzene label. This theory predicts that 23% of the azo label can isomerize at 20 °C. In view of the packing differences and the resulting free volume differences in the chain end vs. the chain center, the relationships between the theoretical value and the experimental values seem reasonable.

We recently utilized azobenzene chromophores as molecular labels in the main chains of amorphous polyurethanes and found that the photoisomerization of such azo labels is very sensitive to the volume changes taking place within the solid film.[1] While photoisomerization in dilute solution occurs by a single rate process, its initial portion in the solid films may be fitted by two separate rate processes. The first is as fast as in dilute solution and is followed by a slower one. The fractional amount of the fast process decreases with physical aging but increases with temperature, plasticization, or glassy deformation.[1b] We suggested that this fraction may be proportional to the number of regions where local free volumes are greater than a critical size necessary for the photoisomerization of the azobenzene group. The azo chromophores in our previous study were attached in the main chain of the amorphous polymers but their location was not specific. In this study, we have incorporated azo chromophores at three specific sites on a polystyrene chain, namely, the chain end, the chain center, or as the side group (see Chart I for their chemical structures). We hoped to observe the differences in the photoisomerization behavior in the glassy state, since the packing efficiency and thus the size distribution of free volumes are expected to depend upon the location of the group on the chain.[2] For example, the chain ends may be associated with more free volume than the center of the chain. The situation in the side group may depend upon the temperature of the glass matrix in relation to the characteristic relaxation temperature for the side-group motion.

With our previous experimental setup in which a xenon arc lamp was used as the irradiation source, the time scale of the photoisomerization measurement was in the hundred of seconds. During such time, free volume may be redistributed as well as decreased to some extent since it is well-known that densification proceeds faster in the initial stage than in the later stage of physical aging.[3] In order to obtain information on the matrix without such uncertainty, it is desirable to carry out time-resolved spectroscopy following short pulses of irradiation.

† This paper is dedicated in honor of Professor Herbert Morawetz.
* Present address: Department of Chemistry, Institute of Materials Science, University of Connecticut, Storrs, CT 06268.

0024-9297/84/2217-1447$01.50/0